Steryl ester formation and accumulation in steroid-degrading bacteria

Johannes Holert[1], Kirstin Brown[1], Ameena Hashimi[1], Lindsay D. Eltis[1], and William W. Mohn[1]

[1]Department of Microbiology & Immunology, Life Sciences Institute, University of British Columbia, Vancouver, British Columbia, Canada

Running title: Bacterial steryl ester synthesis

Correspondence: William W. Mohn, Department of Microbiology & Immunology, Life Sciences Institute, University of British Columbia, 2350 Health Sciences Mall, Vancouver, BC, Canada, V6T 1Z3. Email: wmohn@mail.ubc.ca

ABSTRACT

Steryl esters (SEs) are important storage compounds in many eukaryotes and are often prominent components of intracellular lipid droplets. Here we demonstrate that selected Actino- and Proteobacteria growing on sterols are also able to synthesize SEs and to sequester them in cytoplasmic lipid droplets. We found cholesteryl ester (CE) formation in members of the actinobacterial genera *Rhodococcus*, *Mycobacterium*, and *Amycolatopsis* as well as several members of the proteobacterial Cellvibrionales order. CEs maximally accumulated under nitrogen-limiting conditions, suggesting that steryl ester formation plays a crucial role for storing excess energy and carbon under adverse conditions. *Rhodococcus jostii* RHA1 was able to synthesize phytosteryl and cholesteryl esters, the latter reaching up to 7% of its cellular dry weight and 69% of its lipid droplets. Purified lipid droplets from RHA1 contained CEs, free cholesterol and triacylglycerols (TAGs). In addition, we found formation of CEs in *Mycobacterium tuberculosis* when grown with cholesterol plus an additional fatty acid substrate. This study provides the first evidence for steryl ester accumulation in free-living and pathogenic bacteria and provides a basis for the application of non-pathogenic bacterial whole cell systems in the biotechnological production of SEs for use in functional foods and cosmetics.

IMPORTANCE

Oleaginous bacteria exhibit great potential for the production of high-value neutral lipids, such as triacylglycerols and wax esters. This study describes the formation of steryl esters (SEs) as neutral lipid storage compounds in sterol-degrading oleaginous bacteria, providing a basis for biotechnological production of SEs using bacterial systems with potential applications in the functional food, nutraceutical, and cosmetic industries. We found cholesteryl ester (CE) formation in several sterol-degrading Actino- and Proteobacteria under nitrogen-limiting conditions, suggesting an important role of this process in storing energy and carbon under adverse conditions. In addition, *Mycobacterium tuberculosis* grown on cholesterol accumulated CEs in the presence of an additional fatty acid substrate.

45 **INTRODUCTION**

46

47 Many bacteria synthesize and accumulate carbon and energy storage compounds under
48 environmental stress conditions to increase their survival in environments with fluctuating
49 nutrient conditions (1). A much smaller subset of bacteria are oleaginous and accumulate
50 neutral lipids, namely triacylglycerols (TAGs) and wax esters (WEs), as a prominent class of
51 storage compounds. Although TAG and WE synthesis is rarely described in other bacteria,
52 their accumulation is widespread within the actinobacterial genera *Streptomyces*, *Nocardia*,
53 *Rhodococcus*, *Mycobacterium*, *Dietzia*, and *Gordonia*, and has also been reported in the
54 proteobacterial genera *Acinetobacter*, *Alcanivorax* and *Marinobacter* (2-7). TAGs and WEs are
55 highly hydrophobic, non-polar lipids, which are formed by esterification of a glycerol molecule
56 to three fatty acids or by esterification of a long chain fatty alcohol to a fatty acid, respectively
57 (**Fig. 1**). Potential biotechnological applications of TAG and WE producing bacteria gained
58 increasing attention over the last years due to the considerable industrial relevance of these
59 compounds as biofuels and other products such as feed additives, cosmetics, and lubricants
60 (8). Especially oleaginous *Rhodococcus* strains have been suggested as promising microbial
61 cell factories for the large scale production of neutral lipids due to their ability to convert
62 agroindustrial wastes into valuable lipids and their accessibility to cell engineering for
63 increased lipid production (9).

64 Accumulation of neutral lipids in bacteria is typically induced by environmental stress
65 conditions, in which a suitable carbon source is in excess while additional growth is restricted
66 by a deficiency of other nutrients or environmental conditions. The most prominent example is
67 nitrogen-limitation, which induces TAG and WE synthesis in a wide range of neutral lipid-
68 accumulating Actino- and Proteobacteria. This has been most extensively studied in
69 oleaginous *Rhodococcus* strains, which can accumulate up to 70% of their cellular dry weight
70 as TAGs upon nitrogen depletion, depending on the available carbon source (10-12). In
71 *Mycobacterium tuberculosis*, the causative agent of tuberculosis, dormancy inducing
72 conditions such as nitric oxide (NO) stress or iron-limitation have been shown to initiate
73 accumulation of TAGs and WEs (13, 14). These intracellular carbon and energy storage
74 compounds have been suggested to be important for the pathogenicity of *M. tuberculosis* (15,
75 16).

76 TAGs and WEs are sequestered into cytoplasmic lipid droplets, which are
77 multifunctional organelles encapsulated by a phospholipid monolayer and specific proteins
78 (17). Analogous to oleaginous bacteria, many eukaryotes also sequester neutral lipids as
79 carbon and electron donor reservoirs into cytoplasmic lipid droplets. In contrast to bacterial
80 lipid droplets, many eukaryotic lipid droplets contain sterols in addition to TAGs and WEs (18).
81 Sterols constitute a key class of lipids in most animals, fungi, and plants, where they play

82 essential roles as membrane constituents and precursors for vitamins and steroid hormones.
83 The dominant sterol in animals is cholesterol, while plants have β-sitosterol and other
84 phytosterols, and fungi have ergosterol (**Fig. 1**). Within eukaryotic lipid droplets, the sterol 3-
85 hydroxyl group is typically esterified with fatty acids forming so-called steryl esters (SEs) (**Fig.**
86 **1**), which act as a sterol storage pool. Synthesis and breakdown of SEs plays a vital role in
87 sterol homeostasis and imbalances between free and esterified cholesterol pools are related
88 to several human diseases, such as Wolman disease, cholesteryl ester storage disease,
89 atherosclerosis, and Alzheimer's disease (19). In contrast to eukaryotes, sterol synthesis is
90 rare in bacteria and mainly restricted to *Myxococcales* and *Methylococcales* (20). These
91 bacterial sterols have structural features that distinguish them from eukaryotic sterols (21).
92 Further, it is not known whether these bacteria are able to esterify and store their sterols in
93 lipid droplets.
94 Sterols are abundant growth substrates for bacteria in the environment, and sterol
95 degradation has been characterized in many actinobacterial isolates and is highly conserved
96 in several genera of the Corynebacterineae suborder, namely the genera *Amycolicicoccus,*
97 *Dietzia, Gordonia, Mycobacterium, Nocardia, Rhodococcus,* and *Tsukamurella* (22). In
98 addition, we recently isolated several sterol-degrading strains belonging to the
99 gammaproteobacterial order Cellvibrionales (23), which are also able to degrade sterols such
100 as cholesterol. Under aerobic conditions, sterols are degraded by a conserved pathway into
101 central metabolic moieties such as acetyl-CoA and propionyl-CoA (24), which are
102 subsequently channeled into central metabolic pathways for energy conservation and
103 production of biomass. Among those sterol-degrading bacteria are many that are also well
104 known for their ability to produce TAGs and WEs as neutral lipid storage compounds, such as
105 the Actinobacteria, *Rhodococcus jostii* RHA1 (RHA1) (25) and *Mycobacterium tuberculosis*
106 (*Mtb*) (26). Key enzymes in bacterial TAG and WE synthesis are CoA-dependent, bifunctional
107 WS/DGAT enzymes encoded by *atf* genes. These enzymes catalyze both the acetylation of
108 DAGs to TAGs and of fatty alcohols to WEs (**Fig. 1**) (27). Most WS/DGATs are promiscuous
109 enzymes accepting a variety of acyl-CoAs and alcohols as substrates (5, 28). Interestingly, the
110 WS/DGAT enzyme AtfA from the oleaginous, non-sterol degrading Proteobacterium
111 *Acinetobacter calcoaceticus* ADP1 has been shown to have SE-synthase activity when
112 heterologously expressed in *E. coli* or the yeast *Saccharomyces cerevisiae* (29). Over 50 years
113 ago, two studies reported that different *Mycobacterium* strains produced cholesteryl fatty acid
114 esters when growning with cholesterol (30) and that *Mycobacterium smegmatis* also produced
115 esters of other sterol substrates (31). However, these studies did not provide further insight
116 into the triggering mechanism or cellular localization of SE accumulation and no further reports
117 have been published on bacterial steryl ester synthesis since then.

Here we investigate the ability of sterol-degrading bacteria to synthesize lipid storage compounds from sterol substrates under adverse growth conditions and report formation of SEs as lipid storage compounds in bacteria. This significantly extents the knowledge about bacterial SE formation and provides a basis for biotechnological production of SEs using bacterial systems with potential applications in the functional food, nutraceutical, and cosmetic industries.

125 **RESULTS**

126

127 **Accumulation of SEs in RHA1 under nitrogen-limiting conditions**

128 To investigate formation of lipid-storage compounds from sterol substrates, *Rhodococcus jostii*
129 RHA1 was grown in mineral medium with 1 mM cholesterol or 1 mM of a phytosterol mix,
130 containing 76.4% β-sitosterol, 10.4% β-sitostanol, 7.3% campesterol and 1% campestanol,
131 under nitrogen-limiting and nitrogen-excess conditions. In cholesterol-grown cultures, RHA1
132 reached a biomass in early stationary phase that was approximately four-fold higher under
133 nitrogen-excess than under nitrogen-limiting conditions (**Fig. 2A**). In contrast to the N-excess
134 cultures, the N-limited cultures had no residual ammonium but did have residual cholesterol.
135 Similar results were obtained during growth on the phytosterol substrate mix (not shown). Thin
136 layer chromatography (TLC) analysis of neutral lipid extracts revealed compound spots with
137 the same R_f-value as an authentic cholesterol-palmitate standard (R_f = 0.78) in N-limited
138 cholesterol and phytosterol cultures, but not in the respective N-excess cultures or in N-limited
139 or N-excess cultures grown on non-sterol substrates (**Fig. 2B)**. In addition, compounds with
140 similar Rf-values as an authentic tripalmitin TAG standard (R_f = 0.24) were present in extracts
141 of all N-limited cultures. Time-dependent sampling of RHA1 grown on cholesterol under N-
142 excess and N-limiting conditions revealed that increased formation of the presumptive
143 cholesteryl esters coincided with the depletion of ammonium from the medium (**Fig. 3A**). Under
144 N-excess conditions only minimal amounts of these compounds accumulated during
145 exponential growth and stationary phase (**Fig. 3B**). When nitrogen was replenished in an N-
146 limited, stationary-phase, cholesterol-grown culture, the accumulated lipids including the
147 presumptive SEs disappeared within 72 h (**Fig. 2B**).

148 To confirm the formation of CEs, we analyzed native neutral lipid extracts from strain
149 RHA1 grown with cholesterol or succinate under N-limiting conditions in early stationary phase
150 using a gas chromatography (GC)-coupled flame ionization detector (FID). Comparison to a
151 cholesteryl-palmitate (C16:0) and a cholesteryl-heptadecanoate standard (C17:0) confirmed
152 that these CEs accumulated in cholesterol-grown RHA1 cells (**Fig. 4A**), but were absent in
153 succinate-grown cells. In addition, five other compounds from cholesterol-grown cells eluted
154 close to these CEs, which were absent in succinate-grown cells, suggesting that seven CE
155 species, with different fatty acid chain lengths, are formed with cholesterol as substrate.
156 Comparison to a tripalmitate ($(C16:0)_3$) TAG standard suggested the accumulation of up to
157 nine different TAG species in strain RHA1 grown with cholesterol and eleven different TAG
158 species in cells grown with succinate (**Fig. 4A**). Time-dependent sampling starting at the onset
159 of nitrogen depletion from the media followed by GC-FID analysis showed that the CE:TAG
160 ratio shifted from approximately 60% to 72% within the first 24 h of incubation and to 69% after
161 48 h.

162 To gain further insight into the nature of SEs accumulating in strain RHA1, neutral lipid
163 extracts of cholesterol- and phytosterol-grown cultures were fractionated on silica columns
164 producing five lipid fractions (**supplemental Fig. S1**). SEs eluted in fraction 2 and were well
165 separated from other lipids, like TAGs (Fractions 3 and 4) and free sterols (fractions 5). Aliquots
166 of fraction 2 were subjected to alkaline transesterification with methanol. GC-MS analysis
167 showed that free cholesterol or the free phytosterols (β-sitosterol, β-sitostanol, and
168 campesterol) were formed from transesterification, which were not present in untransesterified
169 extracts (**Fig. 5A-B**). Only the respective sterols provided as a growth substrate were detected
170 in this analysis. In addition, the lack of other free alcohols after transesterification confirmed
171 the absence of wax esters in neutral lipid extracts. In addition, a range of seven fatty acid
172 methyl esters (FAMEs) were detected after transesterification of cholesteryl esters, supporting
173 the results from the GC-FID analysis. Those were identified as methyl esters of C15:0, C16:1,
174 C16:0, C17:1, C17:0, C18:1 and C18:0 (**Fig. 5A**). The most abundant fatty acids were the odd-
175 numbered fatty acids, C17:0, C17:1, and C15:0, which constituted more than 75% of produced
176 FAMEs (**Fig. 5C**). GC-MS analysis of transesterified fraction 2 confirmed that no detectable
177 amounts of other free alcohols indicative of wax esters were present (not shown). Analysis of
178 all neutral lipid extracts using a GC-MS method for wax-ester analysis (32) showed that no
179 detectable amounts of wax esters were present in any sample (not shown), which is in
180 agreement with earlier reports that wax esters are only formed in minimal amounts in RHA1
181 (32).
182 This confirmed that the previously unidentified lipids accumulating in N-limited RHA1
183 cultures grown with cholesterol or phytosterols are fatty acid steryl esters. In the late stationary
184 phase (100 h) CEs accounted for 6.8 +/- 1.4% of the cellular dry weight in N-limited cultures
185 (n = 5 from two independent experiments) based on GC-MS quantification.
186
187 **Localization of accumulated cholesterol and CEs in RHA1**
188 To confirm that accumulating neutral lipids are localized intracellularly, we stained stationary
189 phase, cholesterol-grown, washed, N-excess, and N-limited RHA1 cells with the lipophilic
190 fluorescence stain Nile Red. Microscopic analysis showed that stained lipids accumulated as
191 lipid droplets in the cell interior (**supplemental Fig. S2**) of N-limited cells but were absent from
192 N-excess cells. In addition, we incubated RHA1 with fluorescently labelled cholesterol
193 (BODIPY-cholesterol) and sodium palmitate for 48 h without a nitrogen source. Microscopic
194 analysis showed that fluorescently labelled cholesterol was mainly present within lipid droplets
195 inside the cells (**supplemental Fig. S3**) but mostly absent from cell membranes. TLC analysis
196 of neutral lipid extracts of cells with fluorescently labelled cholesterol showed that no CEs were
197 formed (not shown), which is most likely because the altered chemical structure of the labelled

198 cholesterol side chain inhibits esterification. These results confirm that cholesterol and CEs
199 are mainly stored in intracellular lipid droplets.
200 To gain further insight into the location of CEs within RHA1 cells, lipid droplets were
201 isolated from RHA1 cultures grown with cholesterol or sodium palmitate or a mixture of both
202 substrates under N-limiting conditions. With all three substrate combinations, gradient
203 centrifugation of total cell extracts produced visible bands of lipid droplet on top of the sucrose
204 gradient (**supplemental Fig. S4**). TLC analysis revealed that CEs and free cholesterol were
205 present in neutral lipid extracts of lipid droplets derived from cells grown on cholesterol but not
206 in lipid droplets derived from cells grown on palmitate alone, while TAGs were present under
207 all three conditions (**Fig. 6A**). This was confirmed by fractionation and subsequent
208 transesterification of neutral lipid extracts (not shown). In addition, the lack of other free
209 alcohols after transesterification confirmed the absence of wax esters in lipid droplets. In two
210 independent experiments 52% and 58% of lipids in lipid droplets derived from cells grown on
211 cholesterol were identified as CEs, 31% and 15% as TAGs and 17% and 27% as free
212 cholesterol. Similar results were obtained for lipid droplets derived from cells grown on
213 cholesterol plus palmitate, with 50% and 69% CEs, 35% and 23% TAGs and 15% and 8%
214 cholesterol, while TAGs were the only neutral lipids in lipid droplets derived from cells grown
215 on palmitate (**Fig. 6B**). In lipid droplets from cells grown on cholesterol, between 60% to 70%
216 of fatty acids in CEs and TAGs were odd-numbered (C15 and C17), with C17:0 and C17:1
217 making up around 90% of these fatty acids (**Fig. 6C**). In lipid droplets from cells grown with
218 cholesterol plus palmitate, 23% to 55% of fatty acids were odd-numbered. TAGs of cells grown
219 on palmitate contained almost exclusively (~95%) even-numbered fatty acids. (**Fig. 6C**).
220
221 **Formation of SEs in other sterol-degrading bacteria**
222 To test whether steryl ester formation also occurs in other sterol-degrading bacteria, we
223 extracted neutral lipids from the Actinobacteria, *Mycobacterium smegmatis* strain mc^2155,
224 *Mycobacterium* sp. strain BC8-1, *Rhodococcus opacus* strain Chol-4, *Rhodococcus ruber*
225 strain Chol-4, and *Amycolatopsis* sp. strain ATCC 39116, as well as the
226 Gammaproteobacteria, *Zhongshania* sp. strain SB11-1A, *Haliaceae* sp. strain BC5-1, and the
227 BD1-7 clade bacterium strain SB11-3 grown on cholesterol under nitrogen-limiting and
228 nitrogen-excess conditions. The latter strains were isolated in our lab (23) and are among the
229 first Proteobacteria reported to be able to degrade sterols. TLC analysis indicated these strains
230 produced SEs in N-limited cultures in the stationary phase in differing amounts, with highest
231 yields in the *Rhodococcus*, *Mycobacterium*, and *Zhongshania* strains and lower yields in
232 *Amycolatopsis*, *Haliaceae*, and the BD1-7 clade strain (**supplemental Fig. S5A**). Subsequent
233 fractionation of neutral lipid extracts followed by transesterification and GS-MS analysis
234 confirmed the formation of CEs in all strains (**supplemental Fig. S5B**).

235 In addition, we tested steryl ester formation in *Mycobacterium tuberculosis* (*Mtb*)
236 Erdmann growing on cholesterol and on cholesterol plus sodium palmitate. Because *Mtb* did
237 not grow when sodium palmitate was added to the medium prior to inoculation we spiked
238 palmitate into cultures growing on cholesterol after 5 days. TLC analysis of neutral lipid extracts
239 of *Mtb* indicated the formation of small amounts of CEs in cells growing on cholesterol after 7
240 days and in cells growing on cholesterol plus palmitate after 12 and 13 days, when cells were
241 in stationary phase (**supplemental Fig. S6A-B**). Subsequent fractionation of neutral lipid
242 extracts followed by transesterification and GS-MS analysis confirmed the formation of CEs
243 (**supplemental Fig. S6C**). The only detectable FAME in this fraction was C16:0. Formation of
244 free hexacosanol after transesterification suggested that a C_{26}-OH wax ester was also formed.
245 In addition, we tested whether nitric oxide (NO) stress or iron-limitation, which are known
246 inducers of neutral lipid accumulation in *Mtb* (13, 14), increase CE formation from cholesterol
247 or cholesterol plus palmitate. For this, cholesterol-grown cell suspensions of *Mtb* were
248 incubated with cholesterol alone or cholesterol plus palmitate. To induce NO stress, two pulses
249 of 0.5 mM spermine-NONOate were added at the beginning of the experiment and again after
250 16 h of incubation and samples were taken after 16 h and after 2 days of incubation. Spermine
251 (0.5 mM) was added to control cultures. Deferoxamine (0.5 mM) was added as an iron chelator
252 and samples were taken after 2 and 4 days of incubation. Confirming the results from the initial
253 growth experiment, all extracts from *Mtb* cells incubated with cholesterol plus palmitate
254 contained CEs with C16:0 as only detectable FAME. However, addition of NO or deferoxamine
255 did not increase the amount of accumulating CEs (**supplemental Fig. S6D**). No significant
256 accumulation of CEs occurred in treated cells incubated with only cholesterol. Small amounts
257 of free cholesterol were detected after transesterification of extracts of cell suspensions treated
258 with NO and incubated for 2 days with cholesterol (not shown).

259 **DISCUSSION**

260

261 SEs are important sterol storage compounds in many eukaryotic organisms and are prominent
262 components of some eukaryotic lipid droplets. Here we demonstrate that selected sterol-
263 degrading Actino- and Proteobacteria are also able to synthesize SEs and to sequester them
264 in cytoplasmic lipid droplets. We found steryl ester formation in all sterol-degrading strains
265 investigated in this study, including members of the actinobacterial genera, *Rhodococcus*,
266 *Mycobacterium*, and *Amycolatopsis,* as well as members of the proteobacterial Cellvibrionales
267 order, suggesting that the ability to accumulate excess sterols as an electron donor and carbon
268 source under adverse conditions plays a crucial role in sterol-degrading bacteria. This is
269 supported by findings from the 1960s, which showed that different *Mycobacterium* strains
270 produced steryl esters during growth with sterol substrates (30, 31). The ability of other
271 oleaginous bacteria to synthesize SEs has been overlooked in other studies, which exclusively
272 used non-steroidal substrates, such as glucose, gluconate, or benzoate, when investigating
273 neutral lipid accumulation.

274 Using *Rhodococcus jostii* RHA1 as an oleaginous, sterol-degrading model organism,
275 we found accumulation of minor amounts of CEs during exponential growth on cholesterol
276 when ammonium was available, and a significant increase in CE and TAG accumulation, when
277 ammonium was limiting, indicating that nitrogen-limitation stimulates SE formation. This
278 extends previous reports that nitrogen-limitation is a major inducer for the accumulation of
279 TAGs and WEs in RHA1 with non-steroidal substrates (12, 33). While we found significant
280 accumulation of CEs in the two free-living *Mycobacterium* strains mc^2115 and BC8-1 under
281 nitrogen-limiting conditions with cholesterol as the only substrate, the pathogenic strain
282 *Mycobacterium tuberculosis* (*Mtb*) Erdmann did not grow on cholesterol in nitrogen-limited
283 medium. However, small amounts of cholesterol-palmitate accumulated in this strain when
284 growing on cholesterol plus palmitate as substrates without any stress conditions,
285 demonstrating that pathogenic *Mtb* strains are able to accumulate CEs when a sterol and a
286 fatty acid are available. During infection, *Mtb* triggers formation of foamy macrophages (34,
287 35), which provide a cholesterol and fatty acid-rich microenvironment, and *Mtb* metabolizes
288 these host-derived lipids during infection and persistence (36-38). Interestingly, cholesterol
289 and fatty acid uptake are co-regulated in *Mtb* (39), suggesting that *Mtb* has simultaneous
290 access to both lipid classes *in vivo*. SE synthesis and accumulation could act as a buffer
291 system for excess lipids in *Mtb* providing a way to regulate intracellular lipid metabolism. In
292 addition, SEs could serve as a carbon and electron donor reservoir in *Mtb* under adverse
293 conditions. In a similar manner, TAG accumulation and sequestration in cytoplasmic lipid
294 droplets was shown to occur *in vivo* in pathogenic *Mtb* (16, 40) and was proposed to be
295 important for persistence and reactivation (41). Accumulation of TAGs and WEs was shown to

296 be stimulated by various dormancy-inducing stress conditions, such as hypoxia, NO stress,
297 iron-limitation, and increased acidity, which induce expression of several WS/DGAT encoding
298 genes in *Mtb* (13, 42-44). Although we did not detect increased formation of CEs in *Mtb* under
299 NO stress or iron-limiting conditions, a combination of stress factors as described in (42) might
300 provide deeper insight into the regulation of SE synthesis in *Mtb*.

301 Lipid droplets have been identified in most domains of life, including many eukaryotes,
302 as well as archaeal and bacterial prokaryotes (45). While the general structure of lipid droplets
303 is conserved in all these organisms, comprising a neutral lipid core coated by a phospholipid
304 monolayer and various peripheral proteins, the neutral lipid composition varies significantly
305 between organisms (17, 46). Our results show that CEs, in addition to TAGs and free
306 cholesterol, are sequestered in intracellular lipid droplets in RHA1. The lipid droplet
307 composition in RHA1 grown on cholesterol is very similar to that of lipid droplets found in
308 selected mammalian lipid droplet-producing cell lines (chinese hamster ovaries CHO K2, rat
309 kidney normal NKR and immortalized human fibroblasts SV589) (47), with around 50% CEs,
310 30% TAGs and 20% free cholesterol. The sequestration of cholesterol in lipid droplets is in
311 agreement with an earlier report showing that fluorescently labeled cholesterol predominantly
312 localizes in lipid droplets in mycobacteria (48).

313 Interestingly, the majority of fatty acids stored in TAGs and CEs in cholesterol-grown
314 RHA1 cells were odd-numbered fatty acids, with C17:0 and C17:1 as main fatty acids, which
315 is in stark contrast to the mostly even-numbered fatty acids typically found in eukaryotic neutral
316 lipids. Complete metabolism of one cholesterol molecule through the canonical bacterial 9,10-
317 seco steroid-degradation pathway is proposed to yield four propionyl-CoAs, four acetyl-CoAs,
318 one pyruvate and one succinyl-CoA (24). The preponderance of odd-chain fatty acids in neutral
319 lipids accumulating in RHA1 with cholesterol as carbon source suggests that propionyl-CoA
320 was a significant building block for neutral-lipid fatty acids. Elevated ratios of odd-numbered to
321 even-numbered fatty acids have also been found in TAGs accumulating in RHA1 growing with
322 benzoate under nitrogen-limiting conditions, where propionyl-CoA was presumably generated
323 through the methylmalonyl-CoA pathway from succinate (12). Cholesterol-derived propionyl-
324 CoA has been shown to be toxic to *Mtb* if not metabolized (49), and incorporation of propionyl-
325 CoA into cell wall lipids (50) and TAGs (51) has been suggested as a mechanism to detoxify
326 propionate in *Mtb*. Cholesterol-degrading bacteria, such as RHA1 and *Mtb*, might encounter
327 increased cellular propionyl-CoA levels under adverse growth conditions and the formation of
328 odd-numbered fatty acid CEs might provide an additional sink for this toxic end-product.
329 However, we did not detect odd-numbered fatty acid CEs in *Mtb*, which accumulated CEs in
330 significant amounts only in the presence of an additional fatty acid substrate under the tested
331 conditions.

332 Sterols are abundant growth substrates for bacteria in the environment and sterol
333 degradation is conserved in many actinobacterial genera, particularly in members of the
334 *Corynebacterineae* (22). Recently, we have also identified sterol-degradation in some isolates
335 of the oligotrophic marine Gammaproteobacteria (OMG) group belonging to the Cellvibrionales
336 order (23). Steroid-degrading bacteria are globally distributed and actinobacterial ones are
337 particularly abundant within soil and rhizosphere as well as in deep ocean habitats. Our results
338 indicate that SE formation is conserved in sterol-degrading bacteria, suggesting that this trait
339 might play important roles in these environments. Supporting this hypothesis, most neutral-
340 lipid accumulating Actinobacteria isolated from soil samples (52) belong to taxa in which the
341 ability to degrade sterols is conserved (22) and are thus likely to produce SEs. *De novo*
342 synthesis of sterols is rare in bacteria, being largely restricted to *Myxococcales* and
343 *Methylococcales* (20). Further, it is not known whether these bacteria are able to store these
344 sterols as esters.
345 We searched the genomes of strain RHA1 and of *Mtb* Erdmann for homologs of one
346 prokaryotic and fifty eukaryotic proteins with characterized steryl ester synthase activity
347 available in the Swiss-Prot database, including phosphatidylcholine-sterol *O*-acyltransferases
348 (EC 2.3.1.43), diacylglycerol *O*-acyltransferases (EC 2.3.1.20), sterol *O*-acyltransferase (EC
349 2.3.1.26), and phospholipid:diacylglycerol acyltransferases (EC 2.3.1.158). None of these
350 proteins had any significant similarity (accepted E-values < 0.01) to RHA1 or *Mtb* proteins.
351 Based on the multifunctionality and substrate promiscuity of TAG and WE producing
352 WS/DGAT enzymes, it is feasible that these enzymes might carry out an additional function as
353 steryl ester synthases. Out of the 16 predicted WS/DGATs in RHA1, Atf6 (WP_011594556.1)
354 and Atf8 (WP_011597548.1) have the highest amino acid sequence identity (40% and 39%,
355 respectively) to AtfA from the oleaginous, non-sterol degrading Proteobacterium *Acinetobacter*
356 *calcoaceticus* ADP1, which was shown to have SE-synthase activity when heterologously
357 expressed in *E. coli* or *S. cerevisiae* (29). TAG and WE synthase activities have been
358 confirmed for Atf8 and Atf6, respectively (12, 28) as well as for an Atf6 ortholog in *Rhodococcus*
359 *opacus* PD630 (53), and deletions of the respective genes significantly decreased neutral lipid
360 accumulation. In addition, transcription of *atf8* was strongly induced upon nitrogen depletion in
361 RHA1 growing on benzoate, exhibiting the highest transcript levels of all 16 *atf* genes under
362 nitrogen-limiting conditions (12). In contrast, *atf6* transcripts were most abundant under
363 nitrogen-excess conditions with no apparent transcriptional induction upon nitrogen depletion.
364 WS/DGAT genes identified in soil communities were exclusively from Actinomycetales (54),
365 which includes the steroid-degrading suborder *Corynebacterineae*. In contrast, WS/DGAT
366 genes from marine sediments were exclusively of gammaproteobacterial origin, predominantly
367 from members of the oligotrophic marine Gammaproteobacteria (OMG) group, which have
368 been identified as sterol-degrading (22, 23). BLASTp analysis (max E-value 10^{-15}) of AtfA from

369 *Acinetobacter calcoaceticus* ADP1 against the proteomes of the cholesteryl ester
370 accumulating OMG bacteria *Zhongshania* sp. strain SB11-1A, *Haliaceae* sp. strain BC5-1 and
371 the BD1-7 clade bacterium SB11-3 suggested that these strains encode between four and six
372 WS/DGAT paralogs, further supporting our hypothesis that these proteins might function as
373 steryl ester synthases.

374 Our results indicate that accumulated SEs can be reactivated and degraded in RHA1
375 upon relief of growth-limiting conditions, suggesting that SEs might play a vital role as a carbon
376 and energy reservoir in these environments where fluctuating nutrient availability is common.
377 We searched the genomes of strain RHA1 and of *Mtb* Erdmann for homologs of three
378 prokaryotic and fifteen eukaryotic proteins with characterized or predicted sterol esterase
379 activity available in the TrEMBL and Swiss-Prot databases (EC 3.1.1.13). However, none of
380 the query proteins had significant similarity (accepted coverage > 85%, percent identity > 30%,
381 E-values < 0.01) to RHA1 or *Mtb* proteins. Strain RHA1 encodes up to 54 putative
382 lipases/esterase enzymes (33), which were suggested to contribute to neutral lipid degradation,
383 but no distinct degradation system for endogenous TAGs or WEs has been identified so far.
384 In contrast, the lipase family protein LipY in *M. tuberculosis* has been shown to have TAG
385 degradation activity (55).

386 Interestingly, several animal lineages such as insects and soil-dwelling nematodes
387 have lost the ability to synthesize sterols *de novo* (56) and thus rely on uptake of sterols with
388 their diet (57). It is tempting to speculate that sterol and steryl ester accumulating bacteria in
389 oligotrophic habitats such as soils or freshwater systems might constitute an important source
390 for sterols for bacteriovorous, sterol-auxotrophic eukaryotes such as *Caenorhabditis elegans*
391 or *Daphnia magna.*

392 RHA1 was also able to form esters of the phytosterols β-sitosterol, β-sitostanol, and
393 campesterol under nitrogen-limiting conditions. In recent years, plant-derived phytosterols and
394 their esters were recognized as potential agents to lower serum cholesterol levels in
395 hypercholestemic patients (58, 59) by inhibiting absorption of endogenous and dietary
396 cholesterol in the intestine. Today phytosterols and phytosteryl esters are approved in many
397 countries as safe food additives, and several so-called functional foods are marketed
398 worldwide, which are supplemented with phytosterol and their esters (60). Industrial production
399 of phytosteryl esters is mainly accomplished by chemical esterification or transesterification of
400 plant-derived sterols, which requires high temperatures and the use of strong acids or bases
401 (61). Our study provides a basis for biotechnological production of phytosteryl esters using
402 non-pathogenic whole-cell bacterial systems, thus eliminating the requirement for elevated
403 temperature and acid or base catalysts. Similar to RHA1, many other sterol-degrading
404 Actinobacteria are also able to use phytosterols as growth substrates, providing an excellent
405 screening resource for efficient phytosteryl ester accumulation.
406

407 **MATERIAL AND METHODS**

408

409 **Bacteria and culture conditions**

410 *Rhodococcus jostii* strain RHA1, as well as *Mycobacterium smegmatis* strain mc^{2}155,
411 *Rhodococcus opacus* strain PD630, *Rhodococcus ruber* strain Chol-4, and *Amycolatopsis* sp.
412 strain ATCC 39116 were cultivated in M9 minimal medium supplemented with trace elements
413 and vitamin B1 at 30 °C. The marine bacteria *Mycobacterium* strain BC8-1, *Zhongshania* sp.
414 strain SB11-1A, *Haliaceae* sp. strain BC5-1, and the BD1-7 clade bacterium strain SB11-3
415 were cultivated in artificial marine medium at 21 °C as described earlier (23). Substrates were
416 added at the following concentrations: cholesterol 1 mM, sodium palmitate 1.0 mM or 1.7 mM,
417 succinate 7.0 mM, glucose 5 mM. Starter cultures were grown on 10 mM succinate or 1 mM
418 cholesterol. Cholesterol and other sterol substrates were added as solids and 1% (w/v) methyl-
419 β-cyclodextrin was added to the medium, when required, prior to autoclaving. Substrate
420 removal was monitored by gas chromatography-coupled mass spectrometry (GC-MS) of
421 organic extracts of acidified culture supernatants as described earlier (62). Nitrogen-limiting
422 conditions were achieved by reducing the concentration of ammonium chloride in the medium
423 from 18.70 mM to 0.93 mM. Under N-excess conditions the ratio of carbon to nitrogen in the
424 growth medium was around 1.5:1, while it was 29:1 under N-limiting conditions. To limit
425 nitrogen transfer between cultures, starter cultures were washed twice with phosphate-
426 buffered saline (PBS) without nitrogen. Growth was measured as protein, using the
427 bicinchoninic acid assay (Thermo Scientific) after hot alkaline cell lysis.

428 *Mycobacterium tuberculosis* strain Erdmann (*Mtb*) was grown in 7H9 medium
429 supplemented with 0.5% tyloxapol and 0.5 mM cholesterol at 37 °C. If required 0.5 mM sodium
430 palmitate were spiked into growing cultures after 5 days. Growth was measured as optical
431 density at 600 nm. To test effects of nitric oxide (NO) stress and iron-limitation, cholesterol-
432 grown *Mtb* was harvested and washed in 7H9 medium without carbon source, and cells were
433 suspended in the same medium containing 0.5 mM cholesterol and/or 0.5 mM palmitate. 0.5
434 mM of the NO releasing agent spermine-NONOate was added from a 10 mM stock in 0.01 M
435 NaOH at the beginning of the experiment and again after 16 h of incubation. Spermine was
436 added at the same concentration to control cultures. The iron chelating agent deferoxamine
437 was added at 0.5 mM from a 10 mM stock at the beginning of the experiment.

438 Biosample IDs and references to cholesterol degradation capability of all strains used
439 in this study are summarized in the **supplemental Tab. S1**.

440 **Ammonium quantification**

441 Ammonium concentrations were quantified using indophenol blue. Culture supernatant
442 samples were diluted 25- to 500-fold in distilled water and 200 µl aliquots were distributed into
443 96-well plates in triplicates. 8 µl of reagent (10% w/v phenol in ethanol), 8 µl catalyst (0.5% w/v

444 nitroprusside in water) and 20 µl oxidizing solution (20% w/v trisodium citrate and 1% w/v
445 sodium hydroxide solution, mixed with 5% sodium hypochlorite 4:1 v/v) were added and plates
446 were incubated at 37 °C for 1-2 h in the dark. Absorbance was measured at 630 nm.
447 Ammonium concentrations were calculated using a standard curve with 0-2 mg ml^{-1} ammonium
448 chloride. Alternatively, semi-quantitative ammonium test strips (Quantofix®, Macherey-Nagel,
449 Germany) were used for instant ammonium quantification.

450 **Lipid extraction and analysis**

451 For lipid extraction, cells were harvested, washed twice with distilled water and frozen at -80 °C.
452 *Mtb* cells were autoclaved before freezing. Cell pellets were lyophilized and their dry weight
453 was determined by weighing the pellets. The pellets were then suspended in 1 ml distilled
454 water and broken by bead beating (four rounds of 60 sec at 4.5, 5.0, 5.5, and 6.0 speed setting,
455 respectively, in a FastPrep-24 bead beater; MP Biomedicals, Solon, OH). Between rounds
456 samples were incubated on ice for 5 min. Neutral lipids were extracted with chloroform-
457 methanol (2:1, v/v, 1% acetic acid), dried under nitrogen and suspended in chloroform with 1%
458 acetic acid. If required cholestane was added as internal standard from a 10 mM stock solution
459 in chloroform prior to organic extraction for normalization and quantification of cholesterol and
460 FAMEs. Aliquots of neutral lipid extracts were analyzed by thin layer chromatography (TLC)
461 on 60 F_{254} silica gel plates (Merck) using hexane/diethyl-ether/acetic-acid (90:8:1, v/v/v) as a
462 solvent system. Cholesterol palmitate, cholesterol, tripalmitin, and stearyl-stearate dissolved
463 in chloroform were used as standards. The plates were dried, dabbed with 10% cupric sulfate
464 in 8% phosphoric acid solution and developed at 200 °C for 5-10 min. Native neutral lipid
465 extracts from non-lyophilized cell pellets of strain RHA1 grown under nitrogen-limiting
466 conditions with cholesterol or succinate were also analyzed using a GC-coupled flame
467 ionization detector (FID). For this, 20 ml culture aliquots were harvested, washed twice and
468 frozen at -80°C at different time points after nitrogen was depleted from the medium. Neutral
469 lipids were extracted with tert-butyl ether:methanol (10:3, v/v), followed by two extractions with
470 hexane. Combined organic extracts were dried under nitrogen and suspended in chloroform.
471 Neutral lipid extracts were analyzed by gas chromatography on an Agilent 8890 series GC
472 system equipped with a J&W Select Biodiesel GC Column (15 m, 0.32 mm, 0.10 µm), coupled
473 to a flame ionization detector (FID). GC-injector and detector temperatures were set to 350°C,
474 and 400°C, respectively. 1 µl sample volumes were injected with an initial purge flow rate of
475 50 ml min^{-1}, which subsequently decreased to 20 ml min^{-1} after 2 min, and a septum purge
476 flow rate of 3 ml min^{-1}. The helium flow rate was 8.0972 ml min^{-1}. The oven was set to an initial
477 temperature of 40°C for 2 min with an equilibration time of 0.5 min. The temperature increased
478 by 25°C min^{-1} and was held at 170°C for 2 min, then increased by 15°C min^{-1} to 210°C, then
479 by 5°C min^{-1} to 250°C and held for 5 min. The temperature finally increased by 10°C min^{-1} to
480 400°C and held for 2 min. The FID gas flow settings were set to 400 ml min^{-1} air flow, 30 ml

481 min^{-1} H_2 fuel flow and 25 ml min^{-1} makeup flow (N_2). Cholesteryl palmitate, cholesteryl
482 heptadecanoate, and tripalmitin TAG dissolved in chloroform were used as standards. CE and
483 TAG peaks were normalized with the internal standard cholestane for quantification.

484 **Isolation of lipid droplets**

485 Lipid droplets were isolated as previously described (63, 64). Briefly, RHA1 cultures were
486 harvested by centrifugation (4,000 x g for 10 min), washed three times with 40 ml Buffer A (25
487 mM tricine, 250 mM sucrose, pH 7.8) and suspended in 8 ml buffer A. After incubation on ice
488 for 20 min, cells were disrupted by passing them three times through a cooled French pressure
489 cell at 100 MPa. Cell debris was removed by centrifugation at 4,000 × g for 10 min.
490 Supernatants were loaded into SW40 tubes (Beckman), layered with 2 ml Buffer B (20 mM
491 HEPES, 100 mM KCl, 2 mM MgCl2, pH 7.4), and centrifuged at 180,000 x g for 1 h at 4 °C.
492 The lipid droplet fraction on top of the sucrose gradient was transferred to a 1.5 ml Eppendorf
493 tube and was washed twice with 200 µl Buffer B and finally suspended in 1 ml buffer B. No
494 pellets were formed during washing of the lipid droplets suggesting that lipid droplets were not
495 contaminated by membrane particles. Total lipids were extracted with 5 ml chloroform-acetone
496 (1:1, v/v). The organic phase was dried under nitrogen and lipids were suspended in 1 ml
497 chloroform with 1% acetic acid. Aliquots were analyzed by TLC as described above.

498 **Lipid fractionation**

499 For analyzing the fatty acid profile of cellular lipids and lipid droplets, lipid extracts were
500 fractionated stepwise. Total lipid extracts derived from lipid droplets were first run over a silica
501 column equilibrated with chloroform and neutral lipid fractions were obtained by eluting with 6
502 column volumes chloroform with 1% acetic acid. Glycolipid fractions were subsequently eluted
503 with 6 column volumes acetone (not analyzed further) followed by phospholipid elution with
504 7.5 column volumes methanol. Neutral lipids from lipid droplets and cellular lipid extractions
505 were further fractionated by silica column chromatography. Neutral lipid samples were dried,
506 resuspended in hexane and poured on a silica column equilibrated with the same solvent. 5
507 different fractions were obtained by eluting sequentially with 5 column volumes hexane, 6
508 column volumes hexane/diethyl ether (99:1, v/v), 5 column volumes hexane/diethyl ether (95:5,
509 v/v), 5 column volumes hexane/diethyl ether (92:8, v/v), and 6 column volumes chloroform with
510 1% acetic acid. Fractions were dried under nitrogen and lipids were suspended in 1 ml
511 chloroform with 1% acetic acid. If required, aliquots were analyzed by TLC as described above.

512 **Alkaline transesterification with methanol and lipid quantification**

513 Dried cellular lipid extracts or individual lipid fractions were subjected to alkaline
514 transesterification with methanol modified after (65). For this, dried lipids were resuspended in
515 methanol/toluene (1:1, v/v), mixed with an equal volume of methanolic KOH and incubated for
516 1 h at 50 °C. Phospholipid fractions were incubated for 15 min at 30 °C. Free sterols and fatty
517 acid methyl-esters were extracted twice with 4 volumes hexane/chloroform (4:1, v/v) from 0.15

518 volumes acetic acid (1 M) and 1 volume water. The organic phase was dried under nitrogen
519 and lipids were suspended in 1 ml chloroform with 1% acetic acid. Aliquots were analyzed by
520 GC-MS as described earlier for FAMEs and free cholesterol (62) and for wax esters (32).
521 Cholesterol and fatty acid methyl-esters (FAMEs) were identified by comparison to authentic
522 standards as well as matching against the NIST database (National Institute of Standards and
523 Technology, v11). To quantify total neutral lipids, unfractionated neutral lipid extracts were
524 subjected to transesterification and FAMEs were normalized on cholestane. To quantify SEs
525 in cellular lipid extracts, fractions 1 (containing the internal standard cholestane) and 2
526 (containing steryl esters) were combined prior to transesterification. This allowed normalisation
527 and quantification of free cholesterol derived from transesterification. The percentage of CEs
528 per extracted cellular dry weight was estimated by calculating the total weight of CEs from CE
529 containing fractions and dividing it by the dry weight of the respective extracted cell pellet. For
530 this, the cholesterol concentration in transesterified fractions was calculated using a
531 cholesterol-cholestane standard curve. Subsequently, this was transformed into the total
532 weight of CEs using the molecular masses of all detectable CEs weighted on the peak area
533 ratio of the respective detected FAMEs (C15:0, C16:1, C16:0, C17:1, C17:0, C18:1, C18:0).
534 To estimate ratios of neutral lipid classes in lipid droplets, cholestane and methyl-
535 nonadecanoate were added as internal standards to each fraction prior to transesterification
536 from 10 mM stock solutions in chloroform. Free cholesterol (in fraction 5) and cholesterol
537 released from transesterification of fraction 2 were normalized on cholestane and FAMEs
538 derived from transesterification of CEs and TAGs were normalized on methyl-nonadecanoate
539 before calculating their molar ratios.

540 **Fluorescence microscopy**

541 To localize accumulating neutral lipids in strain RHA1, we added the fluorescent dye Nile Red
542 to growing cholesterol cultures under N-limiting or N-excess conditions without cyclodextrin.
543 Nile red was added to the medium after autoclaving at a final concentration of 0.5 µg ml^{-1} from
544 a sterile stock solution in DMSO (0.3 mg ml^{-1}). Nitrogen and cholesterol depletion were
545 confirmed as described above. Cells from both cultures were examined four days after
546 reaching stationary phase. Cells were washed twice and resuspended in sterile PBS before
547 microscopy. Slides were examined on a Zeiss Axio Imager M1 fluorescence microscope
548 equipped with a Zeiss HBO 103 W/2 high-pressure mercury lamp and an AxioCam MRm
549 camera in phase contrast, differential interference contrast or fluorescence mode.
550 Fluorescence images were shot using excitation and emission wavelengths of 550 nm and
551 605 nm, respectively. All Images were processed using the Zeiss AxioVision software (40 V
552 4.6.3.0).

553 To further analyze the localization of accumulating cholesterol within cells of RHA1
554 under nitrogen-limiting conditions, we performed a cell suspension experiment with

555 fluorescently labeled cholesterol (cholesterol-BODIPY) as substrate under N-limiting
556 conditions followed by laser scanning confocal microscopy. For that, cholesterol-grown cells
557 were washed two times with PBS without nitrogen. Depletion of cholesterol in the starter
558 culture was confirmed by organic extraction and GC-MS analysis. Cells were suspended in
559 1/5 of the original volume of M9 medium without nitrogen containing 0.5 mM palmitate, 0.5 mM
560 fluorescently labeled cholesterol (cholesterol-BODIPY) and 1% (w/v) methyl-β-cyclodextrin
561 and incubated for 48 h at 200 rpm and 30 °C. Cells were washed twice with PBS without
562 nitrogen containing 0.02% (w/v) cholate and 0.02% (v/v) tylaxopol and suspended in PBS.
563 Cells were analyzed using a laser scanning confocal microscope (Olympus Fluoview FV1000-
564 Inverted). A small aliquot of cells was broken by ultrasonication (four rounds of 20 sec using a
565 Microsom cell disruptor XL set to 5; Mandel scientific Co. Ltd., Guelph, ON, Canada) and
566 neutral lipid extracts were analyzed by TLC. Undeveloped plates were analyzed using a GE
567 Typhoon trio + imager with excitation wavelength of 488 nm and an emission filter of 520 nm.
568 Pre-tests with unlabelled cholesterol and palmitate showed that CE accumulation in RHA1 cell
569 suspensions started within 22 h of incubation and continued at least until 95 h of incubation
570 (data not shown).
571

Acknowledgments

We thank Fanrui Meng and Carl Strittmatter for help with fluorescence microscopy. This study was funded by a Discovery Grant from the Natural Sciences and Engineering Research Council of Canada.

Data availability

Draft genomes of *Mycobacterium* strain BC8-1, *Zhongshania* sp. strain SB11-1A, *Haliaceae* sp. strain BC5-1, and the BD1-7 clade bacterium strain SB11-3 have been deposited in the European Nucleotide Archive (ENA) under the BioProject number PRJEB30766.

584 **References**

585

586 1. **J Brigham C**, **Kurosawa K**, **Rha C**, **Sinskey AJ**. 2011. Bacterial carbon storage to
587 value added products. J Microbial Biochem Technol **s3**:1–13.

588 2. **Alvarez HM**, **Steinbüchel A**. 2002. Triacylglycerols in prokaryotic microorganisms.
589 Appl Microbiol Biotechnol **60**:367–376.

590 3. **Russell NJ**, **Volkman JK**. 1980. The effect of growth temperature on wax ester
591 composition in the psychrophilic bacterium *Micrococcus cryophilus* ATCC 15174. J
592 Gen Microbiol **118**:131–141.

593 4. **Kalscheuer R**, **Stöveken T**, **Malkus U**, **Reichelt R**, **Golyshin PN**, **Sabirova JS**,
594 **Ferrer M**, **Timmis KN**, **Steinbüchel A**. 2007. Analysis of storage lipid accumulation
595 in *Alcanivorax borkumensis*: Evidence for alternative triacylglycerol biosynthesis
596 routes in bacteria. J Bacteriol **189**:918–928.

597 5. **Kalscheuer R**, **Steinbüchel A**. 2003. A novel bifunctional wax ester synthase/acyl-
598 CoA:diacylglycerol acyltransferase mediates wax ester and triacylglycerol
599 biosynthesis in *Acinetobacter calcoaceticus* ADP1. J Biol Chem **278**:8075–8082.

600 6. **Garay LA**, **Boundy-Mills KL**, **German JB**. 2014. Accumulation of high-value lipids in
601 single-cell microorganisms: a mechanistic approach and future perspectives. J Agric
602 Food Chem **62**:2709–2727.

603 7. **Röttig A**, **Strittmatter CS**, **Schauer J**, **Hiessl S**, **Poehlein A**, **Daniel R**, **Steinbüchel**
604 **A**. 2016. Role of wax ester synthase/acyl coenzyme a:diacylglycerol acyltransferase
605 in oleaginous *Streptomyces* sp. strain G25. Appl Environ Microbiol **82**:5969–5981.

606 8. **Röttig A**, **Steinbüchel A**. 2013. Acyltransferases in Bacteria. Microbiol Mol Biol Rev
607 **77**:277–321.

608 9. **Alvarez HM**, **Herrero OM**, **Silva RA**, **Hernández MA**, **Lanfranconi MP**, **Villalba MS**.
609 2019. Insights into the metabolism of oleaginous *Rhodococcus* spp. Appl Environ
610 Microbiol **85**:8075–12.

611 10. **Alvarez HM**, **Mayer F**, **Fabritius D**, **Steinbüchel A**. 1996. Formation of
612 intracytoplasmic lipid inclusions by *Rhodococcus opacus* strain PD630. Arch
613 Microbiol **165**:377–386.

614 11. **Waltermann M**, **Luftmann H**, **Baumeister D**, **Kalscheuer R**, **Steinbüchel A**. 2000.
615 *Rhodococcus opacus* strain PD630 as a new source of high-value single-cell oil?
616 Isolation and characterization of triacylglycerols and other storage lipids. Microbiology
617 **146** :1143–1149.

618 12. **Amara S**, **Seghezzi N**, **Otani H**, **Diaz-Salazar C**, **Liu J**, **Eltis LD**. 2016.
619 Characterization of key triacylglycerol biosynthesis processes in rhodococci. Sci Rep
620 **6**:24985.

621 13. **Daniel J**, **Deb C**, **Dubey VS**, **Sirakova TD**, **Abomoelak B**, **Morbidoni HR**,
622 **Kolattukudy PE**. 2004. Induction of a novel class of diacylglycerol acyltransferases
623 and triacylglycerol accumulation in *Mycobacterium tuberculosis* as it goes into a
624 dormancy-like state in culture. J Bacteriol **186**:5017–5030.

625 14. **Bacon J**, **Dover LG**, **Hatch KA**, **Zhang Y**, **Gomes JM**, **Kendall S**, **Wernisch L**,
626 **Stoker NG**, **Butcher PD**, **Besra GS**, **Marsh PD**. 2007. Lipid composition and

627 transcriptional response of *Mycobacterium tuberculosis* grown under iron-limitation in
628 continuous culture: identification of a novel wax ester. Microbiology **153**:1435–1444.

629 15. **Stehr M**, **Elamin AA**, **Singh M**. 2013. Lipid inclusions in mycobacterial infections.
630 Tuberculosis - Current Issues in Diagnosis and Management, Bassam H. Mahboub
631 and Mayank G. Vats, IntechOpen, doi: 10.5772/54526

632 16. **Garton NJ**, **Christensen H**, **Minnikin DE**, **Adegbola RA**, **Barer MR**. 2002.
633 Intracellular lipophilic inclusions of mycobacteria in vitro and in sputum. Microbiology
634 **148**:2951–2958.

635 17. **Zhang C**, **Liu P**. 2017. The lipid droplet: A conserved cellular organelle. Protein &
636 Cell **8**:796–800.

637 18. **Ruggles KV**, **Turkish A**, **Sturley SL**. 2013. Making, baking, and breaking: The
638 synthesis, storage, and hydrolysis of neutral lipids. Annu Rev Nutr **33**:413–451.

639 19. **Korber M**, **Klein I**, **Daum G**. 2017. Steryl ester synthesis, storage and hydrolysis: A
640 contribution to sterol homeostasis. Biochim Biophys Acta **1862**:1534–1545.

641 20. **Wei JH**, **Yin X**, **Welander PV**. 2016. Sterol synthesis in diverse bacteria. Front
642 Microbiol **7**:990.

643 21. **Lee AK**, **Banta AB**, **Wei JH**, **Kiemle DJ**, **Feng J**, **Giner J-L**, **Welander PV**. 2018. C-
644 4 sterol demethylation enzymes distinguish bacterial and eukaryotic sterol synthesis.
645 Proc Natl Acad Sci USA **115**:5884–5889.

646 22. **Bergstrand LH**, **Cardenas E**, **Holert J**, **Van Hamme JD**, **Mohn WW**. 2016.
647 Delineation of steroid-degrading microorganisms through comparative genomic
648 analysis. MBio **7**:e00166–16.

649 23. **Holert J**, **Cardenas E**, **Bergstrand LH**, **Zaikova E**, **Hahn AS**, **Hallam SJ**, **Mohn**
650 **WW**. 2018. Metagenomes reveal global distribution of bacterial steroid catabolism in
651 natural, engineered, and host environments. MBio **9**: e02345-17.

652 24. **Crowe AM**, **Casabon I**, **Brown KL**, **Liu J**, **Lian J**, **Rogalski JC**, **Hurst TE**, **Snieckus**
653 **V**, **Foster LJ**, **Eltis LD**. 2017. Catabolism of the last two steroid rings in
654 *Mycobacterium tuberculosis* and other Bbacteria. MBio **8**:e00321–17.

655 25. **van der Geize R**, **Yam K**, **Heuser T**, **Wilbrink MH**, **Hara H**, **Anderton MC**, **Sim E**,
656 **Dijkhuizen L**, **Davies JE**, **Mohn WW**, **Eltis LD**. 2007. A gene cluster encoding
657 cholesterol catabolism in a soil actinomycete provides insight into *Mycobacterium*
658 *tuberculosis* survival in macrophages. Proc Natl Acad Sci USA **104**:1947–1952.

659 26. **Wipperman MF**, **Sampson NS**, **Thomas ST**. 2014. Pathogen roid rage: cholesterol
660 utilization by *Mycobacterium tuberculosis*. Crit Rev Biochem Mol Biol **49**:269–293.

661 27. **Alvarez HM**. 2016. Triacylglycerol and wax ester-accumulating machinery in
662 prokaryotes. Biochimie **120**:28–39.

663 28. **Barney BM**, **Wahlen BD**, **Garner E**, **Wei J**, **Seefeldt LC**. 2012. Differences in
664 substrate specificities of five bacterial wax ester synthases. Appl Environ Microbiol
665 **78**:5734–5745.

666 29. **Kalscheuer R**, **Luftmann H**, **Steinbüchel A**. 2004. Synthesis of novel lipids in
667 *Saccharomyces cerevisiae* by heterologous expression of an unspecific bacterial
668 acyltransferase. Appl Environ Microbiol **70**:7119–7125.

669 30. **Schubert K**, **Kaufmann G**. 1965. Bildung von Sterinestern in der Bakterienzelle.
670 Biochim Biophys Acta **106**:592–597.

671 31. **Schubert K**, **Kaufmann G**, **Hörhold C**. 1969. Veresterung von Sterinen mit
672 Fettsäuren und mit Bernsteinsäure in *Mykobakterien*. Biochim Biophys Acta **176**:163–
673 169.

674 32. **Round J**, **Roccor R**, **Li S-N**, **Eltis LD**. 2017. A fatty acyl-CoA reductase promotes
675 wax ester accumulation in *Rhodococcus jostii* RHA1. Appl Environ Microbiol
676 **83**:e00902–17–12.

677 33. **Hernández MA**, **Mohn WW**, **Martínez E**, **Rost E**, **Alvarez AF**, **Alvarez HM**. 2008.
678 Biosynthesis of storage compounds by *Rhodococcus jostii* RHA1 and global
679 identification of genes involved in their metabolism. BMC Genomics **9**:600.

680 34. **Peyron P**, **Vaubourgeix J**, **Poquet Y**, **Levillain F**, **Botanch C**, **Bardou F**, **Daffé M**,
681 **Emile J-F**, **Marchou B**, **Cardona P-J**, **de Chastellier C**, **Altare F**. 2008. Foamy
682 macrophages from tuberculous patients' granulomas constitute a nutrient-rich
683 reservoir for *M. tuberculosis* persistence. PLoS Pathog **4**:e1000204.

684 35. **Russell DG**, **Cardona P-J**, **Kim M-J**, **Allain S**, **Altare F**. 2009. Foamy macrophages
685 and the progression of the human tuberculosis granuloma. Nat Immunol **10**:943–948.

686 36. **VanderVen BC**, **Fahey RJ**, **Lee W**, **Liu Y**, **Abramovitch RB**, **Memmott C**, **Crowe**
687 **AM**, **Eltis LD**, **Perola E**, **Deininger DD**, **Wang T**, **Locher CP**, **Russell DG**. 2015.
688 Novel inhibitors of cholesterol degradation in *Mycobacterium tuberculosis* reveal how
689 the bacterium's metabolism is constrained by the intracellular environment. PLoS
690 Pathog **11**:e1004679.

691 37. **Pandey AK**, **Sassetti CM**. 2008. Mycobacterial persistence requires the utilization of
692 host cholesterol. Proc Natl Acad Sci USA **105**:4376–4380.

693 38. **Muñoz Elías E**, **Upton A**, **Cherian J**, **McKinney JD**. 2006. Role of the methylcitrate
694 cycle in *Mycobacterium tuberculosis* metabolism, intracellular growth, and virulence.
695 Mol Microbiol **60**:1109–1122.

696 39. **Nazarova EV**, **Montague CR**, **La T**, **Wilburn KM**, **Sukumar N**, **Lee W**, **Caldwell S**,
697 **Russell DG**, **VanderVen BC**. 2017. Rv3723/LucA coordinates fatty acid and
698 cholesterol uptake in *Mycobacterium tuberculosis*. Elife **6**:678.

699 40. **Daniel J**, **Maamar H**, **Deb C**, **Sirakova TD**, **Kolattukudy PE**. 2011. *Mycobacterium*
700 *tuberculosis* uses host triacylglycerol to accumulate lipid droplets and acquires a
701 dormancy-like phenotype in lipid-loaded macrophages. PLoS Pathog **7**:e1002093.

702 41. **Low KL**, **Rao PSS**, **Shui G**, **Bendt AK**, **Pethe K**, **Dick T**, **Wenk MR**. 2009.
703 Triacylglycerol utilization is required for regrowth of in vitro hypoxic nonreplicating
704 *Mycobacterium bovis* bacillus Calmette-Guerin. J Bacteriol **191**:5037–5043.

705 42. **Deb C**, **Lee C-M**, **Dubey VS**, **Daniel J**, **Abomoelak B**, **Sirakova TD**, **Pawar S**,
706 **Rogers L**, **Kolattukudy PE**. 2009. A novel in vitro multiple-stress dormancy model
707 for *Mycobacterium tuberculosis* generates a lipid-loaded, drug-tolerant, dormant
708 pathogen. PLoS ONE **4**:e6077.

709 43. **Sirakova TD**, **Deb C**, **Daniel J**, **Singh HD**, **Maamar H**, **Dubey VS**, **Kolattukudy PE**.
710 2012. Wax ester synthesis is required for *Mycobacterium tuberculosis* to enter in vitro
711 dormancy. PLoS ONE **7**:e51641.

712 44. **Sirakova TD**, **Dubey VS**, **Deb C**, **Daniel J**, **Korotkova TA**, **Abomoelak B**,
713 **Kolattukudy PE**. 2006. Identification of a diacylglycerol acyltransferase gene
714 involved in accumulation of triacylglycerol in *Mycobacterium tuberculosis* under
715 stress. Microbiology **152**:2717–2725.

716 45. **Murphy DJ**. 2011. The dynamic roles of intracellular lipid droplets: from archaea to
717 mammals. Protoplasma **249**:541–585.

718 46. **Waltermann M**, **Steinbüchel A**. 2005. Neutral lipid bodies in prokaryotes: Recent
719 insights into structure, formation, and relationship to eukaryotic lipid depots. J
720 Bacteriol **187**:3607–3619.

721 47. **Bartz R**, **Li W-H**, **Venables B**, **Zehmer JK**, **Roth MR**, **Welti R**, **Anderson RGW**, **Liu**
722 **P**, **Chapman KD**. 2007. Lipidomics reveals that adiposomes store ether lipids and
723 mediate phospholipid traffic. J Lipid Res **48**:837–847.

724 48. **Faletrov Y**, **Brzostek A**, **Plocinska R**, **Dziadek J**, **Rudaya E**, **Edimecheva I**,
725 **Shkumatov V**. 2016. Uptake and metabolism of fluorescent steroids by
726 mycobacterial cells. Steroids **117**:29–37.

727 49. **Griffin JE**, **Pandey AK**, **Gilmore SA**, **Mizrahi V**, **McKinney JD**, **Bertozzi CR**,
728 **Sassetti CM**. 2012. Cholesterol catabolism by *Mycobacterium tuberculosis* requires
729 transcriptional and metabolic adaptations. Chem Biol **19**:218–227.

730 50. **Russell DG**, **VanderVen BC**, **Lee W**, **Abramovitch RB**, **Kim M-J**, **Homolka S**,
731 **Niemann S**, **Rohde KH**. 2010. *Mycobacterium tuberculosis* wears what it eats. Cell
732 Host Microbe **8**:68–76.

733 51. **Singh A**, **Crossman DK**, **Mai D**, **Guidry L**, **Voskuil MI**, **Renfrow MB**, **Steyn AJC**.
734 2009. *Mycobacterium tuberculosis* WhiB3 maintains redox homeostasis by regulating
735 virulence lipid anabolism to modulate macrophage response. PLoS Pathog
736 **5**:e1000545–16.

737 52. **Hauschild P**, **Röttig A**, **Madkour MH**, **Al-Ansari AM**, **Almakishah NH**, **Steinbüchel**
738 **A**. 2017. Lipid accumulation in prokaryotic microorganisms from arid habitats. Appl
739 Microbiol Biotechnol **101**: 2203–2216.

740 53. **Alvarez AF**, **Alvarez HM**, **Kalscheuer R**, **Waltermann M**, **Steinbüchel A**. 2008.
741 Cloning and characterization of a gene involved in triacylglycerol biosynthesis and
742 identification of additional homologous genes in the oleaginous bacterium
743 *Rhodococcus opacus* PD630. Microbiology **154**:2327–2335.

744 54. **Lanfranconi MP**, **Alvarez AF**, **Alvarez HM**. 2015. Identification of genes coding for
745 putative wax ester synthase/diacylglycerol acyltransferase enzymes in terrestrial and
746 marine environments. AMB Express **5**:42.

747 55. **Deb C**, **Daniel J**, **Sirakova TD**, **Abomoelak B**, **Dubey VS**, **Kolattukudy PE**. 2006. A
748 novel lipase belonging to the hormone-sensitive lipase family induced under
749 starvation to utilize stored triacylglycerol in *Mycobacterium tuberculosis*. J Biol Chem
750 **281**:3866–3875.

751 56. **Desmond E**, **Gribaldo S**. 2009. Phylogenomics of sterol synthesis: insights into the
752 origin, evolution, and diversity of a key eukaryotic feature. Genome Biol Evol **1**:364–
753 381.

754 57. **Wollam J**, **Antebi A**. 2011. Sterol regulation of metabolism, homeostasis, and
755 development. Annu Rev Microbiol **80**:885–916.

58. **Weingärtner O**, **Böhm M**, **Laufs U**. 2008. Controversial role of plant sterol esters in the management of hypercholesterolaemia. Eur Heart J **30**:404–409.

59. **Lichtenstein AH**, **Deckelbaum RJ**. 2001. AHA Science Advisory. Stanol/sterol ester-containing foods and blood cholesterol levels. A statement for healthcare professionals from the Nutrition Committee of the Council on Nutrition, Physical Activity, and Metabolism of the American Heart Association. Circulation **103**:1177–1179.

60. **Bacchetti T**, **Masciangelo S**, **Bicchiega V**, **Bertoli E**, **Ferretti G**. 2011. Phytosterols, phytostanols and their esters: from natural to functional foods. Mediterr J Nutr Metab **4**:165–172.

61. **He W-S**, **Zhu H**, **Chen Z-Y**. 2018. Plant Sterols: Chemical and Enzymatic Structural Modifications and Effects on Their Cholesterol-Lowering Activity. J Agric Food Chem **66**:3047–3062.

62. **Casabon I**, **Crowe AM**, **Liu J**, **Eltis LD**. 2013. FadD3 is an acyl-CoA synthetase that initiates catabolism of cholesterol rings C and D in actinobacteria. Mol Microbiol **87**:269–283.

63. **Ding Y**, **Yang L**, **Zhang S**, **Wang Y**, **Du Y**, **Pu J**, **Peng G**, **Chen Y**, **Zhang H**, **Yu J**, **Hang H**, **Wu P**, **Yang F**, **Yang H**, **Steinbüchel A**, **Liu P**. 2012. Identification of the major functional proteins of prokaryotic lipid droplets. J Lipid Res **53**:399–411.

64. **Ding Y**, **Zhang S**, **Yang L**, **Na H**, **Zhang P**, **Zhang H**, **Wang Y**, **Chen Y**, **Yu J**, **Huo C**, **Xu S**, **Garaiova M**, **Cong Y**, **Liu P**. 2013. Isolating lipid droplets from multiple species. Nat Protoc **8**:43–51.

65. **Ichihara K**, **Yamaguchi C**, **Nishijima H**, **Saito K**. 2003. Preparation of FAME from sterol esters. J Amer Oil Chem Soc **80**:833–834.

782 **Figure legends**
783
784 **Fig. 1:** Schematic representation of triacylglycerols (TAGs) and wax esters (WEs) as neutral
785 lipid storage compounds in bacteria and of a cholesterol-ester. Structures of the major animal,
786 plant, and fungal sterols cholesterol, β-sitosterol, and ergosterol.
787
788 **Fig. 2:** Growth of strain RHA1 under nitrogen-limiting and nitrogen-excess conditions. **A)** at
789 early stationary phase (around 100 h). **B)** TLC analysis of neutral lipid extracts from early
790 stationary phase N-limited (-N) and N-excess (+N) cultures grown with different carbon
791 sources. Abbreviations: CP, cholesterol palmitate; C, cholesterol; TAG, triacylglycerols; Ph,
792 phytosterol mix; S, succinate; P, pyruvate; G, glucose; NH_4^+, N replenished in stationary-phase
793 C-N culture. The volume of neutral lipid extracts applied to TLC plates was normalized on the
794 extracted cellular dry weight of each culture. Red arrows indicate standard spots. Results were
795 obtained on two TLC plates which were treated exactly the same way throughout the
796 experiment. The results of one representative experiment out of several biological and
797 technical replicates are shown for each substrate.
798
799 **Fig. 3:** Growth of RHA1 on 1 mM cholesterol under nitrogen-limiting conditions **(A)** and
800 nitrogen-excess conditions **(B)**. The volume of neutral lipid extracts applied to TLC plates was
801 normalized on the basis of culture biomass as protein. One of two reproducible experiments is
802 shown.
803
804 **Fig. 4:** GC-FID analysis of accumulating neutral lipids in nitrogen-limited RHA1 cultures grown
805 with cholesterol or succinate. **(A)** GC-FID chromatograms of authentic cholesteryl palmitate
806 (C16:0) and cholesteryl heptadecanoate (C17:0) standards (blue line) and of a trimpalmitin
807 TAG ($C16:0_3$) standard (orange line) and of neutral lipid extracts of cholesterol- and succinate-
808 grown cells harvested 24 h after nitrogen depletion. Seven accumulating CE species were
809 identified either by comparison to the standards or based on the proximity of their respective
810 peaks to the standard peaks and their absence in succinate grown cells. Identified and
811 predicted CEs are labelled with blue arrows, identified and predicted TAG species are labelled
812 with orange arrows. **(B)** Ratio of accumulating CEs (blue bars) and TAGs (orange bars) in
813 cholesterol-grown nitrogen-limited RHA1 cultures over time starting at nitrogen depletion (0 h).
814 Peak areas of the seven CE- and nine TAG-peaks shown in Fig. 4A were normalized on the
815 peak area of the internal standard cholestane (not shown) before calculating their respective
816 sums. Average values of three biological replicates and their standard deviations are shown.
817
818 **Fig. 5:** Identification of SEs accumulating in N-limited RHA1 cultures. GC-MS analysis of
819 transesterified fraction 2 (black peaks) and untreated fraction 2 (grey peaks) of neutral lipid

820 extracts of nitrogen-limited cultures grown with **(A)** cholesterol and **(B)** phytosterols.
821 Transesterification of SEs produced free cholesterol and the free phytosterols β-sitosterol, β-
822 sitostanol, and campesterol, as well as seven fatty acid methyl esters of C15:0, C16:1, C16:0,
823 C17:1, C17:0, C18:0 and C18:1. One representative GC-MS chromatogram is shown. **(C)** Fatty
824 acid profile of transesterified fraction 2 derived from nine cholesterol-grown cultures grown
825 under nitrogen-limiting conditions from five independent experiments harvested approximately
826 24h after nitrogen depletion. Odd-numbered fatty acids are coloured blue and even-numbered
827 fatty acids are coloured red
828
829 **Fig. 6:** Isolation of lipid droplets from strain RHA1 grown with cholesterol (**C**) or palmitate (**P**)
830 or a mixture of cholesterol plus palmitate (**C+P**) under nitrogen-limiting conditions. **A)** TLC
831 analysis of neutral lipids derived from total lipid extracts from isolated lipid droplets.
832 Abbreviations as in previous figures. **B)** Molar ratio of TAGs, CEs and free cholesterol in lipid
833 droplets derived from cholesterol, cholesterol plus palmitate and palmitate grown cells. **C)**
834 Ratio of even to odd-numbered fatty acids in CEs and TAGs in lipid droplets and the respective
835 contributing fatty acid chain lengths. The results of two independent experiments (I and II) are
836 shown in **B)** and **C)** and of experiment II in **A)**.
837

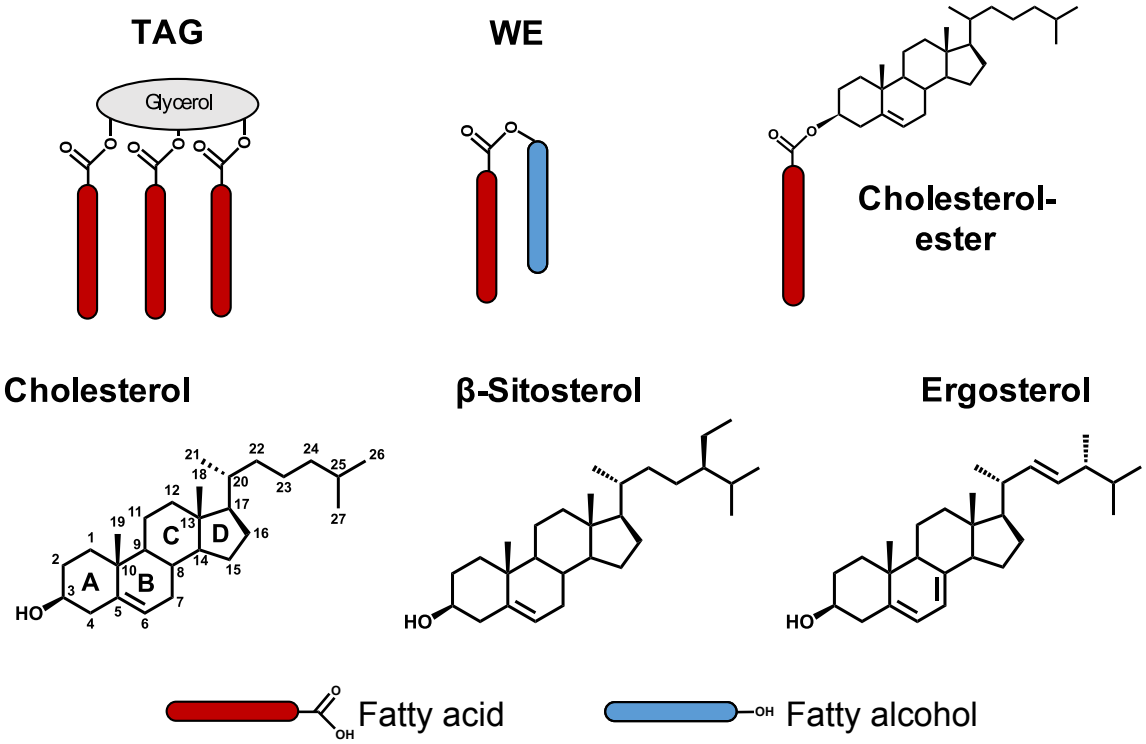

Fig. 1: Schematic representation of triacylglycerols (TAGs) and wax esters (WEs) as neutral lipid storage compounds in bacteria and of a cholesterol-ester. Structures of the major animal, plant, and fungal sterols cholesterol, β-sitosterol, and ergosterol.

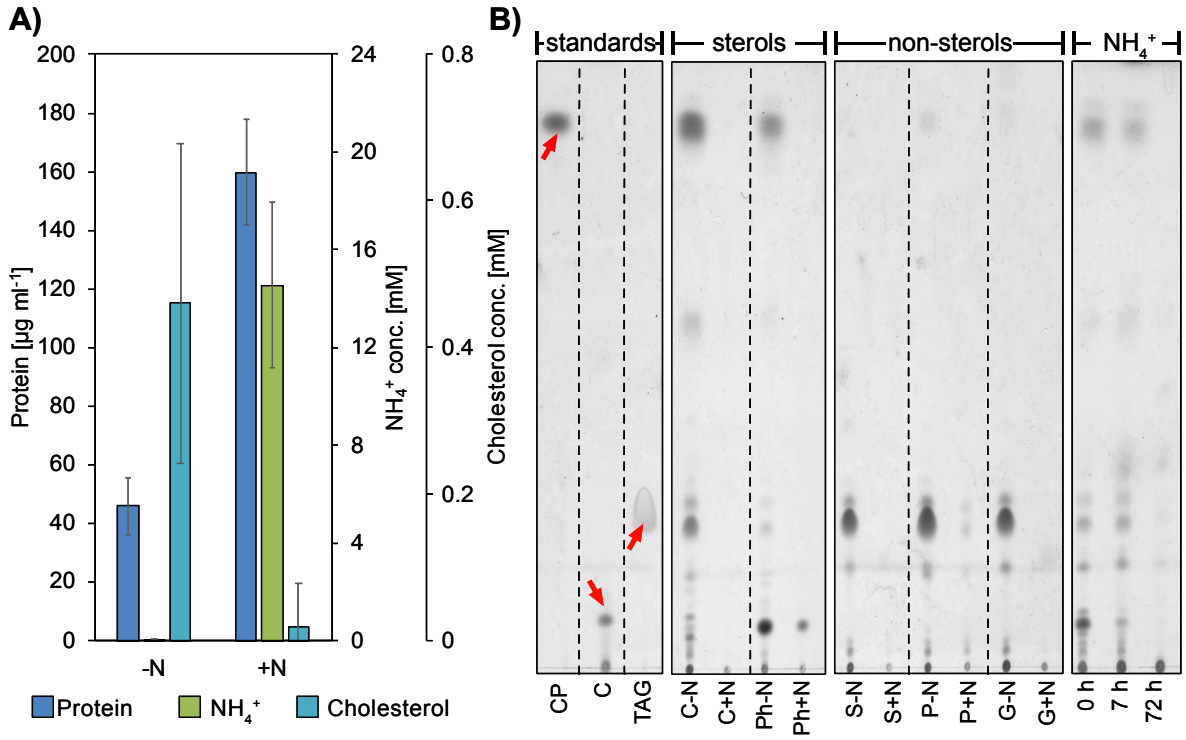

Fig. 2: Growth of strain RHA1 under nitrogen-limiting and nitrogen-excess conditions. **A)** at early stationary phase (around 100 h). **B)** TLC analysis of neutral lipid extracts from early stationary phase N-limited (-N) and N-excess (+N) cultures grown with different carbon sources. Abbreviations: CP, cholesterol palmitate; C, cholesterol; TAG, triacylglycerols; Ph, phytosterol mix; S, succinate; P, pyruvate; G, glucose; NH_4^+, N replenished in stationary-phase C-N culture. The volume of neutral lipid extracts applied to TLC plates was normalized on the extracted cellular dry weight of each culture. Red arrows indicate standard spots. Results were obtained on two TLC plates which were treated exactly the same way throughout the experiment. The results of one representative experiment out of several biological and technical replicates are shown for each substrate.

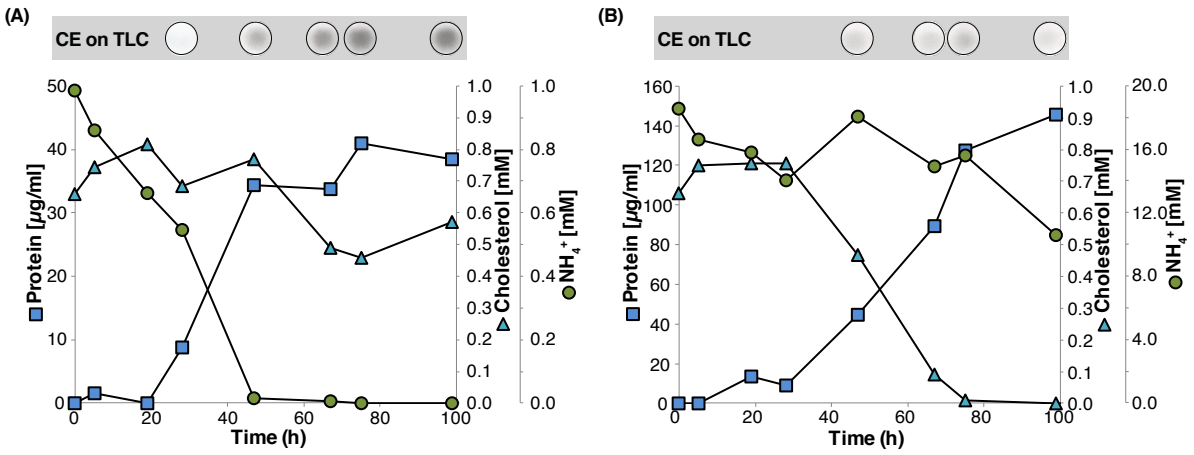

Fig. 3: Growth of RHA1 on 1 mM cholesterol under nitrogen-limiting conditions **(A)** and nitrogen-excess conditions **(B)**. The volume of neutral lipid extracts applied to TLC plates was normalized on the basis of culture biomass as protein. One of two reproducible experiments is shown

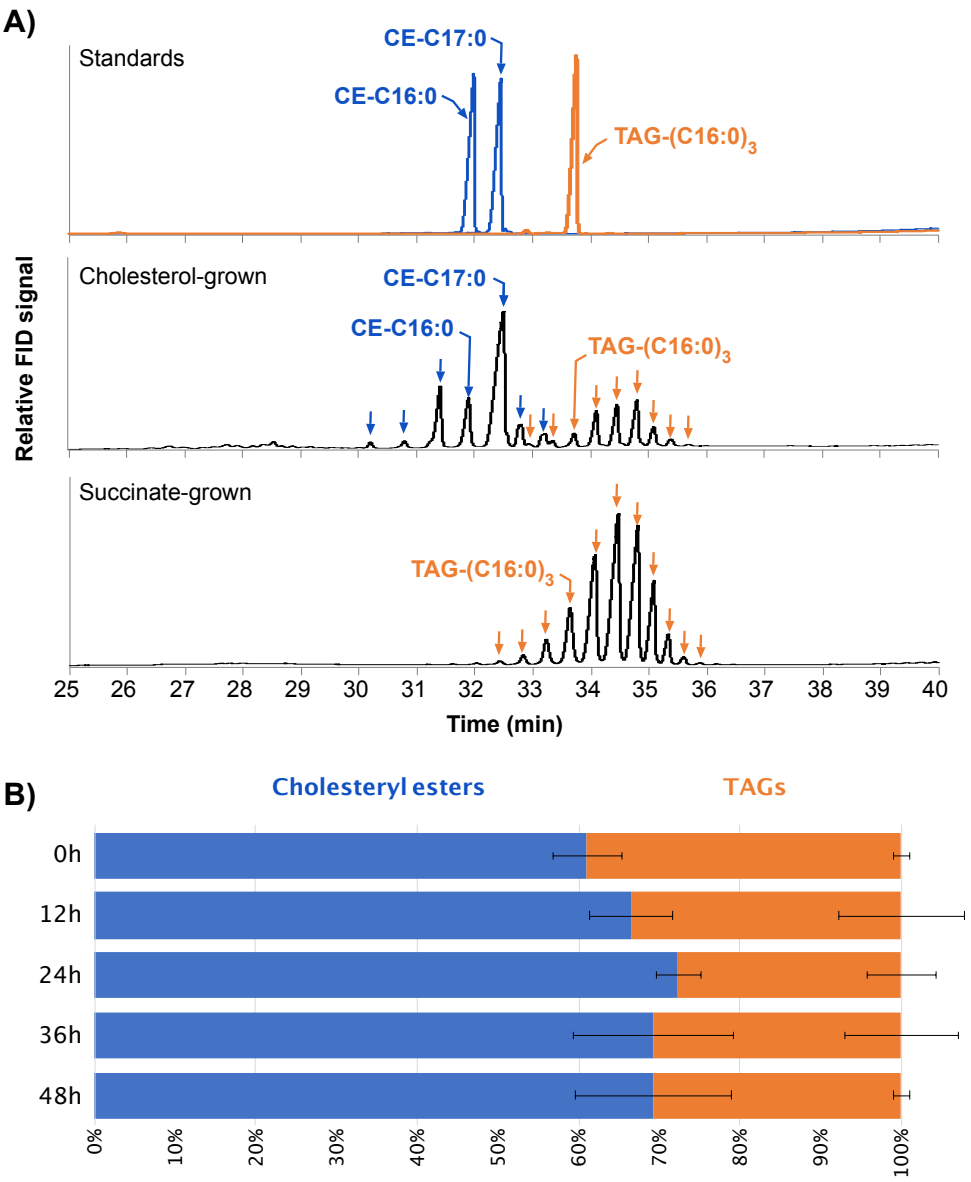

Fig. 4: GC-FID analysis of accumulating neutral lipids in nitrogen-limited RHA1 cultures grown with cholesterol or succinate. **(A)** GC-FID chromatograms of authentic cholesteryl palmitate (C16:0) and cholesteryl heptadecanoate (C17:0) standards (blue line) and of a tripalmitin TAG ($C16:0_3$) standard (orange line) and of neutral lipid extracts of cholesterol- and succinate-grown cells harvested 24 h after nitrogen depletion. Seven accumulating CE species were identified either by comparison to the standards or based on the proximity of their respective peaks to the standard peaks and their absence in succinate grown cells. Identified and predicted CEs are labelled with blue arrows, identified and predicted TAG species are labelled with orange arrows. **(B)** Ratio of accumulating CEs (blue bars) and TAGs (orange bars) in cholesterol-grown nitrogen-limited RHA1 cultures over time starting at nitrogen depletion (0 h). Peak areas of the seven CE- and nine TAG-peaks shown in Fig. 4A were normalized on the peak area of the internal standard cholestane (not shown) before calculating their respective sums. Average values of three biological replicates and their standard deviations are shown.

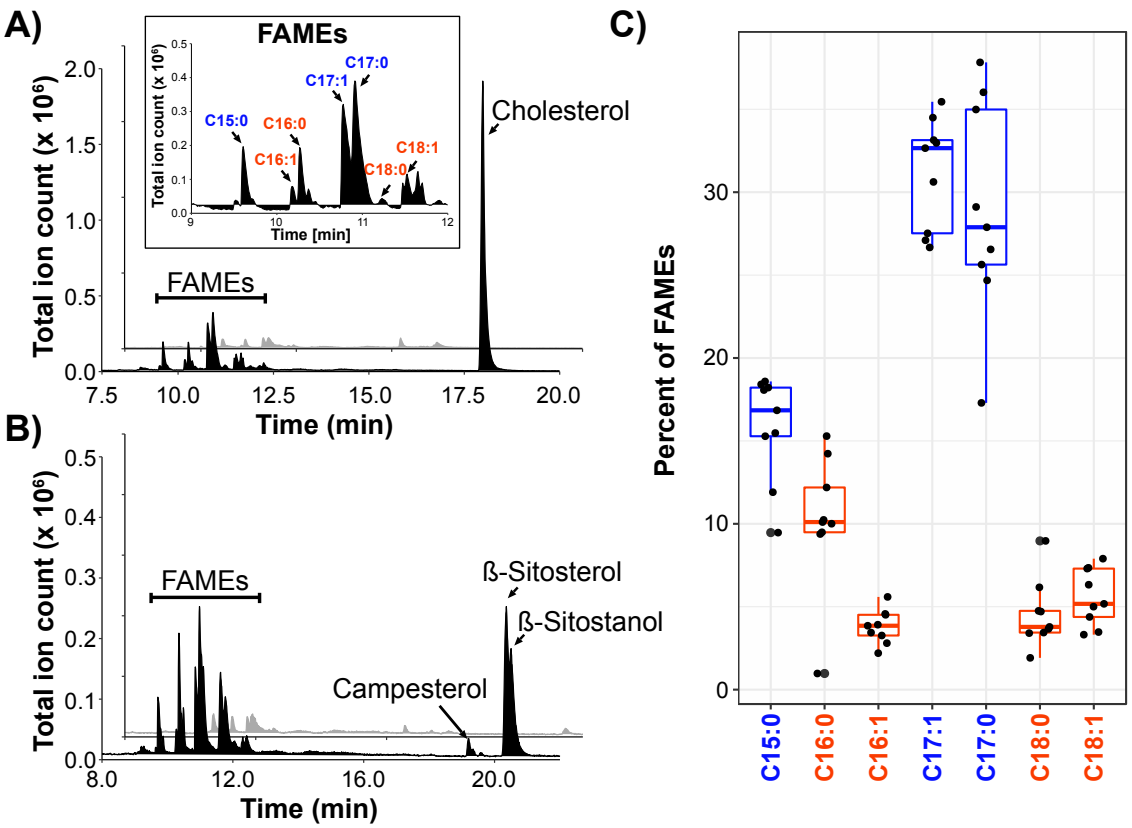

878

879 **Fig. 5:** Identification of SEs accumulating in N-limited RHA1 cultures. GC-MS analysis of
880 transesterified fraction 2 (black peaks) and untreated fraction 2 (grey peaks) of neutral lipid
881 extracts of nitrogen-limited cultures grown with **(A)** cholesterol and **(B)** phytosterols.
882 Transesterification of SEs produced free cholesterol and the free phytosterols β-sitosterol, β-
883 sitostanol, and campesterol, as well as seven fatty acid methyl esters of C15:0, C16:1, C16:0,
884 C17:1, C17:0, C18:0 and C18:1. One representative GC-MS chromatogram is shown. **(C)** Fatty
885 acid profile of transesterified fraction 2 derived from nine cholesterol-grown cultures grown
886 under nitrogen-limiting conditions from five independent experiments harvested approximately
887 24h after nitrogen depletion. Odd-numbered fatty acids are coloured blue and even-numbered
888 fatty acids are coloured red

889

890

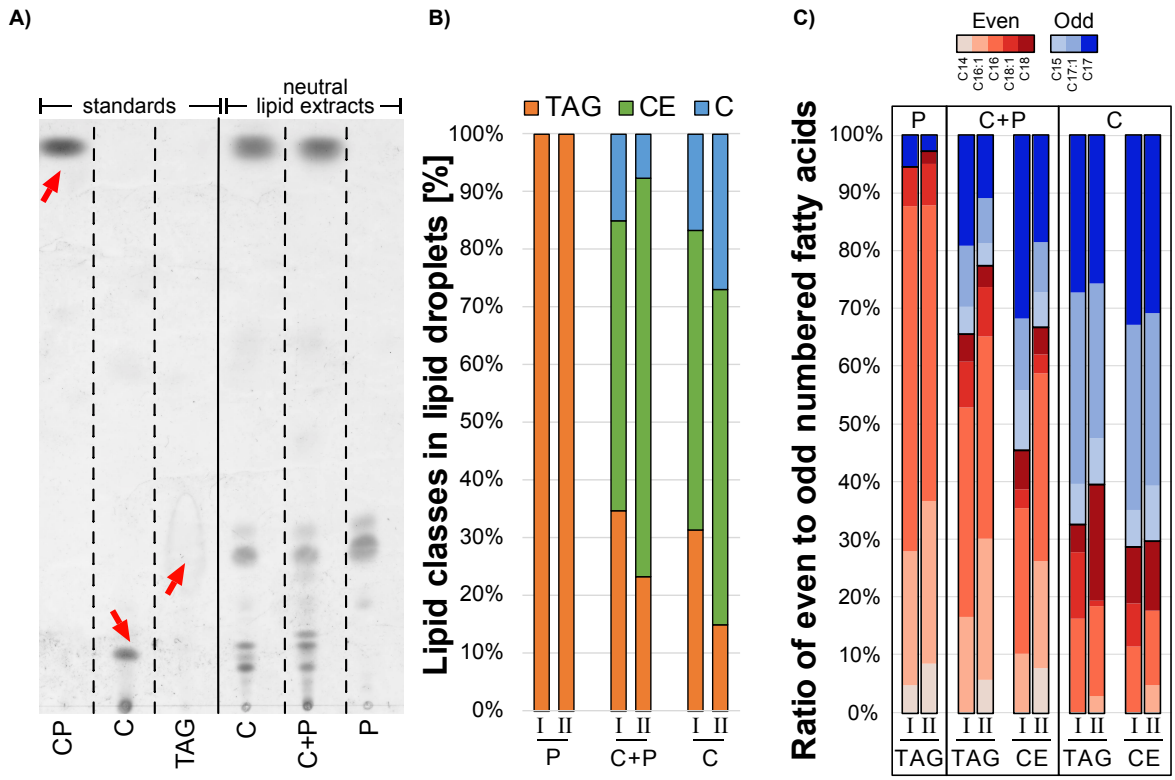

Fig. 6: Isolation of lipid droplets from strain RHA1 grown with cholesterol (**C**) or palmitate (**P**) or a mixture of cholesterol plus palmitate (**C+P**) under nitrogen-limiting conditions. **A)** TLC analysis of neutral lipids derived from total lipid extracts from isolated lipid droplets. Abbreviations as in previous figures. **B)** Molar ratio of TAGs, CEs and free cholesterol in lipid droplets derived from cholesterol, cholesterol plus palmitate and palmitate grown cells. **C)** Ratio of even to odd-numbered fatty acids in CEs and TAGs in lipid droplets and the respective contributing fatty acid chain lengths. The results of two independent experiments (I and II) are shown in **B)** and **C)** and of experiment II in **A)**.